Review Article

Natural Biomolecules in Leaves and Fruit Extracts Mediate the Biosynthesis of SnO_2 Nanoparticles: A Mini Review

Irmaizatussyehdany Buniyamin[1,3*], Muhamad Faizal Abd Halim[1], Kevin Alvin Eswar[3,4], Kathleen J. Jalani[5], Syed Abdul Illah Alyahya Syed Abd Kadir[6], Maryam Mohammad[1,3,7], Mohd Yusri Idorus[8], Noor Asnida Asli[1,3], Mohamad Rusop Mahmood[1,2], Zuraida Khusaimi[1,3*]

[1]NANO-SciTech Laboratory, Centre for Functional Materials and Nanotechnology (FMN), Institute of Science, Universiti Teknologi MARA (UiTM), 40450 Shah Alam Selangor, Malaysia
[2]NANO-ElecTronic Centre, Engineering College, Universiti Teknologi MARA (UiTM), 40450 Shah Alam, Selangor, Malaysia
[3]Faculty of Applied Sciences, Universiti Teknologi MARA (UiTM), 40450 Shah Alam Selangor, Malaysia
[4]Faculty of Applied Sciences, Universiti Teknologi MARA (UiTM) Sabah Branch Tawau Campus, 91032 Tawau Sabah Malaysia
[5]Faculty of Pharmacy, Universiti Teknologi Mara (UiTM), 42300 Bandar Puncak Alam, Selangor, Malaysia
[6]Pusat Asasi Universiti Teknologi MARA (UiTM) Cawangan Selangor, Kampus Dengkil, 43800 Dengkil Selangor, Malaysia
[7]Faculty of Applied Sciences, Universiti Teknologi MARA (UiTM) Perak Branch Tapah Campus, 35000 Tapah Road Perak, Malaysia
[8]Institute Medical Molecular Biotechnology (IMMB), Faculty of Medicine, Universiti Teknologi MARA, Jalan Hospital, 47000 Sungai Buloh Selangor, Malaysia

ABSTRACT

The green approach of nanoparticle preparation via biosynthesis method is known to be more economical, less toxic, and environmental-friendly as compared to the conventional chemical and physical methods which are hazardous and expensive. The advantages that are offered by this nanoscale material are their high surface area to volume ratio and the great stability which drive the performance to be effective. Among several nanoparticles, metal oxide namely tin (iv) oxide nanoparticles (SnO_2 NPs) have attracted significant attention in recent years specifically in the nanotechnology discipline due to its wide applications in medical, catalysis, energy storage, coatings, sensors, dye-sensitized solar cells, and optoelectronics. The biosynthesis method was reported to be conducted using an aqueous extract of the green part of the plant, mostly the leaves and fruit segment. Within these plant parts, rich amounts of natural biomolecules are available that are capable of mediating the synthesis mechanism through capping and reducing action, which involves the chelating activity. Several characterization techniques were carried out to determine their unique characteristics in terms of crystallinity and morphological aspects such as XRD, TEM, SEM, EDX, FTIR, and UV-Vis. This paper summarizes the biosynthesis works of SnO_2 NPs using leaves and fruit extract, and their properties were tested based on the photocatalytic performance as well as biomedical activities such as antimicrobial, antibacterial, antioxidant, and cytotoxicity.

Keywords: Biomolecules, Green synthesis, Nanotechnology, Tin (iv) oxide nanoparticles, Applications

Corresponding authors
Irmaizatussyehdany Buniyamin
NANO-SciTech Laboratory,
Centre for Functional Materials and Nanotechnology (FMN),
Institute of Science, Universiti Teknologi MARA (UiTM),
40450 Shah Alam Selangor, Malaysia
syehdany@uitm.edu.my

Copyright© 2023 UiTM Press. This is an open access article licensed under CC BY-SA
https://creativecommons.org/licenses/by-sa/4.0/

Zuraida Khusaimi
NANO-SciTech Laboratory,
Centre for Functional Materials and Nanotechnology (FMN),
Institute of Science, Universiti Teknologi MARA (UiTM),
40450 Shah Alam Selangor, Malaysia
zurai142@uitm.edu.my

Received: 15 March 2023; accepted: 27 Oct 2023
Available online: 15 Nov 2023
http://doi.org/10.24191/IJPNaCS.v6i2.03

1.0 Introduction

Nanotechnology is the characterization, design, and application of a combination of systems, structures, and devices by size control as well as the shape of particles at the scale of 10^{-9} m. Their brilliant characteristics are unquestionable when the particles are scaled down to the nanoscale compared to the bulk size (1-2). Through controlling and manipulating the nanoparticles (NPs), an enhancement in terms of unique physical, chemical, and magnetic properties can be obtained. These unique properties stimulated researchers' interest in synthesizing nanoscale materials with different shapes, sizes, and compositions. There has been extensive research on synthesizing and optimizing nanoparticles (3-7).

Previously, many physical and chemical synthetic routes have been developed (8-11). To overcome the drawbacks of chemical synthesis, a new bio-mediated green synthesis technique, namely the biosynthesis method has been introduced and it is more helpful than chemical synthesis. It is free from toxic solvents and chemicals; does not involve high-cost equipment, reproducible, easy to handle, and cost-effective (12-13). Among the nanoparticles, tin (iv) oxide nanoparticles (SnO_2 NPs) have been studied intensively because of their potential applicability to lithium-ion batteries, transparent conducting electrodes in ionic devices, anti-reflective coatings, solid-state gas sensors, solar cells, catalytic support materials, energy storage, medicals, etc. (Figure 1) (14-16). The preparation of SnO_2 NPs using conventional methods reported to suffer from several drawbacks such as hydrothermal, solvothermal, microwave synthesis, co-precipitation, sol-gel, spray pyrolysis, chemical vapor deposition, thermal evaporation of oxide powders, rapid oxidation of elemental tin and microemulsion (17-18).

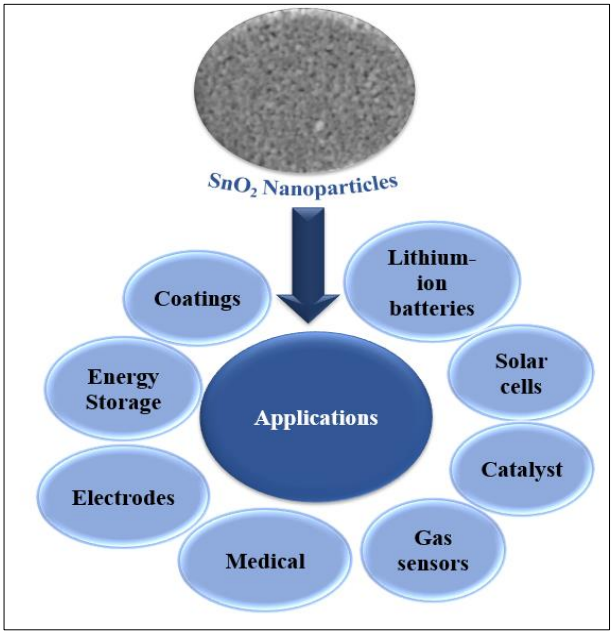

Figure 1: The extensive potential of SnO_2 NPs underlies their broad spectrum of applications.

Herein, this study discusses the biosynthesis of SnO_2 NPs using green plant parts, which are leaves and fruit, with their respective applications based on the properties possessed by the purely biosynthesized SnO_2 NPs It is hypothesized that biomolecules (bioactive compounds or phytochemicals) present in this plant extracts are polyphenolic flavonoids alkaloids, phenolic acids, polyphenols, proteins, sugars, and terpenoids to role as the capping and reducing agent towards tin cation (20-21). In general, the extraction process involves the boiling process under temperatures between 40 to 70^oC in water or organic solvent to soften and break down the plant cell thus releasing the soluble functionalized biomolecule (Figure 2) (22). By having a polar solvent, the extraction of the polar phenolic biomolecules can be optimized thus maximizing the availability reducing agent (23). Later, the reduced metal ions may be engaged with atmospheric oxygen or oxygen from the degrading phytochemicals forming metal oxide nanoparticles. Furthermore, the biomolecules exist in the synthesis stage able to avoid the agglomerate between the particles thus the formation of the nanoparticles is dispersedly-formed hence increasing the high surface area to volume ratio (9, 24-25). The general procedure to prepare SnO_2 NPs is shown in Figure 2.

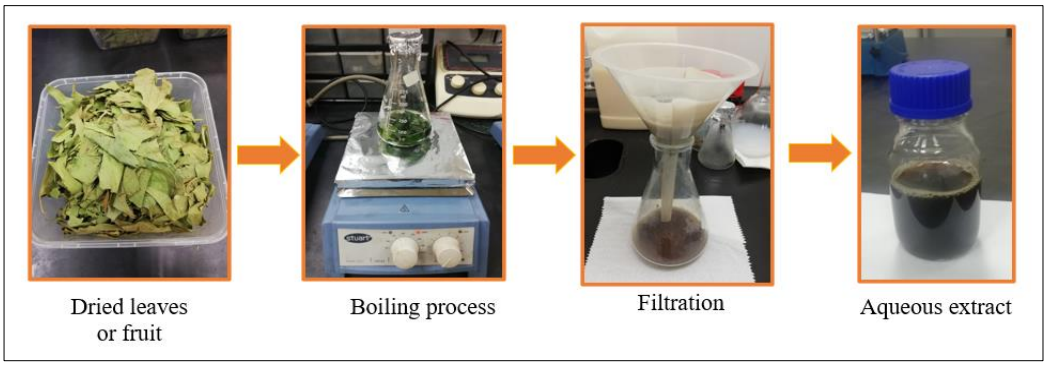

Figure 2: The standard method for obtaining an aqueous extract involves taking dried leaves or fruits, boiling them in water at a temperature range of 60-80°C for approximately 20-30 minutes, and then filtering the mixture through Whatman paper to obtain the final extract.

2.0 Plausible reaction mechanism of SnO_2 NPs

The biocompatible mechanism of SnO_2 NPs formation is presumably initiated when the solution of the salt precursor was mixed with aqueous extract of leaves or fruits as shown in Figure 3. The cation of tin (Sn^{4+}) dispenses in the solution and forms the complex with hydroxyl groups of biomolecules, that is believed to be actively functionalized through chelation activity. The possible biomolecules that are likely to be taken into account in the mechanism are the polyphenolic biomolecules, which contain adjacent hydroxyl groups in the aromatic ring to assist the capping action. In general, a tetravalent network of Sn^{4+} with two units of hydroxyl groups originating from two different biomolecules was built up when Sn^{4+} was used as the precursor salt. At this stage, the biomolecules keep their group from being agglomerate among themselves, and finally, SnO_2 NPs were furnished after the complex of the biomolecule-tin cation was calcined under thermal treatment (9, 26-32). The proposed mechanism for the formation of SnO_2 NPs is shown in Figure 4.

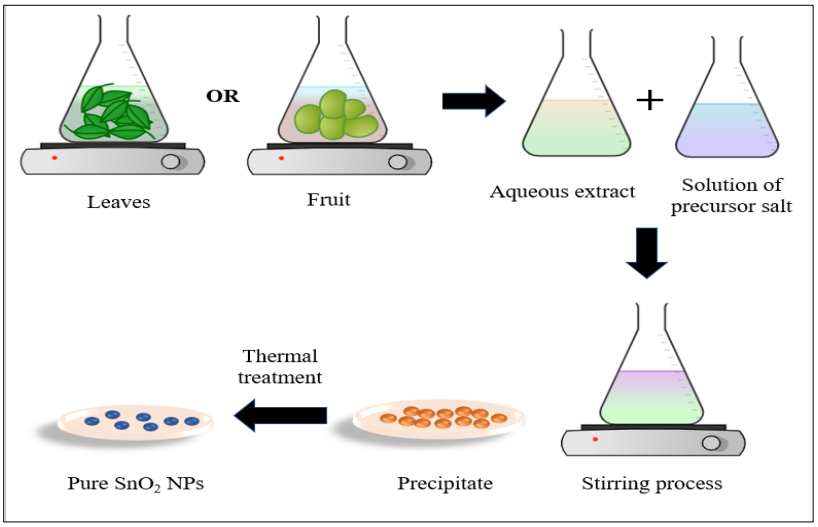

Figure 3: The biosynthesis of SnO_2 NPs using an aqueous extract of leaves and fruits typically follows a general procedure, which involves the mixing of the extract solution with a precursor salt solution until a precipitate form. This precipitate contains biomolecules that act as capping agents for the intermediate SnO_2 NPs. Subsequently, the resulting mixture undergoes thermal treatment through a calcination process.

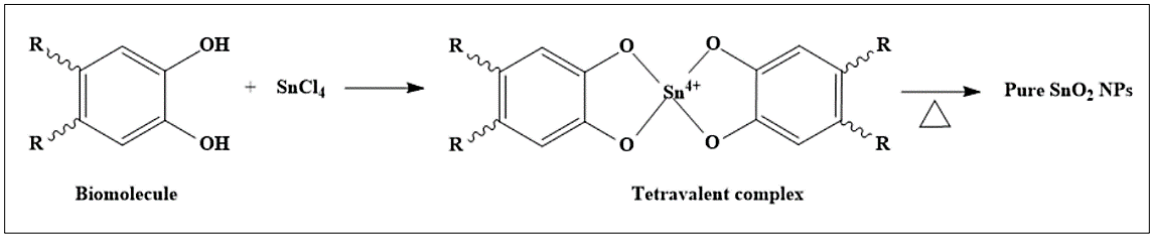

Figure 4: Proposed mechanism for SnO_2 NPs formation; The formation of a tetravalent complex occurs due to the biomolecules' capping action, which also contributes to stabilization of the intermediate SnO_2 NPs.

3.0 Biosynthesis of SnO_2 Nanoparticles

3.1 The utilization of leaf extract in the mediating synthesis

During the process of collecting samples for extraction, leaf samples appeared as a popular choice of plant fragments. This is mainly due to their abundantly available, ease of collection, non-toxic nature, and handy storage. Many researchers have utilized leaf extracts to successfully produce pure SnO_2 NPs. To synthesize nonporous nanocrystalline SnO_2 NPs with a large surface area, Haq et al. used a leaf extract from *Daphne mucronata* (32). The hydroxyl groups contained in coumarins, coumarino lignans, flavonoids, carboxylic acids, lignin, and triterpenoids were believed to act as both capping and reducing agents. The analysis using X-ray diffraction (XRD) resulted in a crystallite size of 15 nm; while scanning electron microscopy (SEM) provided evidence of an average SnO_2 NPs size of 64 nm. Photocatalytic testing demonstrated that in the presence of SnO_2 photocatalyst, about 99 % of Rhodamine-6G was degraded within 390 minutes, with a degradation rate of 1.48×10-2 min-1. The photocatalytic activity of SnO_2 NPs was found to be improved with

increasing irradiation time under simulated sunlight. The antimicrobial efficiency of SnO_2 NPs was tested on several types of microbes using the agar well diffusion method. The activity was assessed by measuring the zones of inhibition in millimetres at each concentration and volume. The result demonstrated high efficacy in inhibiting Gram-negative bacteria (GNB) compared to Gram-positive bacteria (GPB) and fungi. Additionally, the activity was observed to enhance when higher concentrations of SnO_2 NPs and volumes were applied. In conclusion, the antimicrobial action of SnO_2 NPs was caused by the formation of H_2O_2, which entered the cell and destroyed the cytoplasm of the organism.

Moreover, an extract of *Pruni spinosae flos* utulized to synthesize SnO_2 NPs by Dobrucka *et al*. (33). The authors identified two biomolecules, namely flavonoids and phenolic acid to be responsible for the chelation activity in the synthesis mechanism. These biomolecules were found in high concentrations and contained biologically-active hydroxyl groups. Fourier transform infrared (FTIR) analysis of SnO_2 NPs results indicated the presence of the Sn-O-Sn group at region 400 cm^{-1}. UV-Visible (UV-Vis) analysis showed maximum absorption at 408 nm as a sign of the clustered nature of the pure SnO_2 NPs. The result from transmission electron microscopy (TEM) observed the nanoparticles to agglomerate into larger particles, with a size of approximately 9 nm. Energy-dispersive X-ray spectroscopy (EDS) showed Sn peaks between 0 to 5 kV, proving the high purity of SnO_2 NPs. The synthesized SnO_2 NPs were then tested for their ability and activity through antibacterial activity analysis and cytotoxic activity analysis. The antibacterial test was determined by the minimal bactericidal concentration (MBC) and the minimal fungicidal concentration (MFC), which showed that the synthesized SnO_2 NPs nanoparticles had a good biocidal effect on all tested microorganisms. The studies on cytotoxic activity also demonstrated that the SnO_2 NPs nanoparticles led to cell death; however, this impact was highly dependent on the concentration and was time-dependent.

Calotropis gigantea aqueous leaf extract was used by Bhosale et al. to create SnO_2 NPs (34). The study confirmed that biomolecules were present in the extract by doing an analysis of FTIR, such as amines, aldehydes, hydroxyl, and aromatic ring groups, in which authors suggested acting as a capping agent. Qualitative phytochemical screening was also conducted to confirm the presence of flavonoids, tannins, saponins, terpenoids, alkaloids, and phenols in the leaf extract. XRD analysis discovered that the biosynthesized SnO_2 NPs exhibited a tetragonal structure with a size of 35 nm. Additionally, SEM analysis indicated a mixed morphology with insignificant agglomeration. The photocatalytic activity of the synthesized SnO_2 NPs was calculated based on the degradation of Methyl orange under UV-visible light, whereby the results recorded 80% degradation within 3 hours.

A water-based extract from cauliflower leaf (*Brassica oleracea L. var. botrytis*) was used in a green technique by Osuntokun *et al*. (35). The authors stated that the tin cation interacted with biomolecules, that is antioxidants belonging to the polyphenol and flavonoid groups through the chelation process. This chelation process formed a bivalent complex between the biomolecules and the tin cation. The obtained precipitate was later annealed at temperatures of 300 and 450^{o}C for two hours. XRD analysis indicated that both samples exhibited a tetragonal rutile phase, with sizes approximately to be 3.1 and 6.1 nm, and these findings were supported by TEM results. UV-Vis spectroscopy discovered that the synthesized SnO_2 NPs exhibited quantum confinement, with

absorption peaks showing a blue shift compared to bulk SnO_2. Besides, photoluminescence (PL) spectroscopy demonstrated emission maxima corresponding to lower band gap energy light irradiation. For photocatalytic testing, both samples degraded about 91 % and 88 % of methylene blue within 180 minutes. This higher degradation was recorded when using smaller particle sizes of SnO_2 NPs that were prepared at an annealing temperature of 300^{o}C rather than 450^{o}C.

Green tea extract, namely *Camellia sinensis*, was used by Selvakumari *et al*. in a work to create SnO_2 NPs (36). The researchers theorized that the four types of polyphenolic flavanol derivatives contain in green tea, namely epicatechin (EC), epigallocatechin (EGC), picatechin gallate (ECG), and epigallocatechin gallate (EGCG), would be an active reducing and stabilizing agents. These biomolecules are highly water soluble and polar, with a good ability to donate both protons and electrons in the reaction mechanism. The results indicated that as the annealing temperature increased, the crystallite size of the nanoparticles also increased. XRD analysis revealed that the crystallite size was less than 20 nm. Furthermore, a morphological investigation using SEM showed that the particles displayed a spherical shape, with sizes ranging from 5 to 30 nm.

Another research utilizing extracts derived from *Camellia sinensis* leaves was conducted by Luque et al., in which the experiment involved varying concentrations of the extract (37). The researchers proposed that biomolecules present in the leaf extract, such as flavonoids, amino acids, proteins, and enzymes, effectively functioned as chelating and capping agents. In particular, the hydroxyl groups of polyphenols and flavonoids are biomolecules having the ability to coordinate with the tin cation. The analysis using SEM revealed that the synthesized SnO_2 NPs showed a quasi-spherical shape, with average sizes of 6.91, 5.2, and 4.7 nm. XRD results indicated a hexagonal structure in the rutile phase, with an interplanar distance (d) of 0.33 nm. The photocatalytic testing recorded a complete degradation when methylene blue and rhodamine-B were employed, while for methyl orange about 81% of degradation was recorded.

Utilizing guava (*Psidium guajava*) leaf extract, Kumar *et al*. showed the production of SnO_2 NPs using a basic, affordable, and ecologically friendly technique (38). The extract was believed to contain diverse categories of biomolecules that aided this bio-based synthesis, which are phenolic compounds, flavonoids, sesquiterpene alcohols, and triterpenoid acids. The size of the synthesized SnO_2 NPs was discovered using TEM, in which the nanoscale ranges from 8 to 10 nm. The photocatalytic testing recorded the efficient degradation ability of SnO_2 NPs on RY186 dye, whereby within a time length of 180 minutes, 90% of the dye was degraded and gave a rate constant of 0.00476 min^{-1}.

Furthermore, an extract obtained from *Aspalathus linearis* was used by Diallo et al. in synthesizing SnO_2 NPs (39). The suggested biomolecules responsible for the chelating action were identified as aspalathin (a dihydrochalcone glycoside), as well as related chalcone compounds including nothofagin and aspalalinin. The authors also mentioned that the leaf powder was mixed with water for two days to ensure the maximum extraction of the required biochemicals. The thermal treatment was carried out at temperatures of 400 ^{o}C, 700 ^{o}C, and 900^{o}C, to give quasi-spherical and fully spherical morphologies. From HRTEM results, the average diameter of the synthesized SnO_2 NPs was found to be in the range of 2.1 to 19.3 nm. Remarkably, the smallest SnO_2 NPs exhibited excellent

photocatalytic activity by effectively degrading three dyes namely methylene blue, congo red, and eosin Y.

An easy one-pot hydrothermal method was described in a work by Fu et al. on the biosynthesis of SnO_2 NPs utilising *Plectranthus amboinicus* (40). It was believed that in the formation of SnO_2 NPs, the biomolecules present in the extract served as the reducing agent. Authors claimed a similar function of the extract in the formation of Ag NPs based on the former report, however the specific name for the biomolecules was not exposed. The average size of the synthesized SnO_2 NPs was recorded to be 63 nm, which resulted from SEM analysis. From the characterizations using XRD and EDX, it was indicated that the proposed procedure led to high-purity SnO_2 NPs, whereas XRD analysis resulted in the existence of a tetragonal structure of SnO_2 NPs. Besides, the biosynthesized SnO_2 NPs demonstrated an efficient performance in degrading about 95% of rhodamine-B within 120 minutes. Additionally, SnO_2 NPs sustained their functionality at 91% even after enduring five consecutive cycles.

Additionally, Wicaksono and his team used leaves extract from *Amaranthus tricolour L* to perform a biofabrication technique to create SnO_2 NPs (41). The researchers proposed that several biomolecules, which are gallic acid (3,4,5-OH), myrcetin, quercetin-3-O-rutinoside (rutin), and apigenin-7-O-glucoside (apigetrin) to be responsible for reducing the tin cation during the synthesis. XRD analysis revealed the polycrystalline nature of the powder with a rutile structure, and the crystallite size was recorded to be 18 nm. SEM analysis showed that the nanoparticles displayed a spherical shape. Moreover, EDS measurements proved the occurrence of Sn as the major element. TEM analysis demonstrated an irregular particle distribution with diameters within the range of 20 to 40 nm. Regarding the photodegradation ability of the SnO_2 nanoparticles on Bromophenol blue, it was observed that complete degradation was achieved when H_2O_2 was added, while in its absence only half degradation was recorded.

The creation of SnO_2 NPs using *Cleistanthus collinus* methanolic leaf extract was also reported by Kamaraj *et al.* (42). They believe the natural biomolecules that exist in the leaves would aid the reducing action such as cleistanthin A and cleistanthin B, which lay under the category of lignan lactone glucosides. From XRD analysis, SnO_2 NPs were recorded as a tetragonal lattice structure with a grain size of 49 nm while SEM gave nanoscale measurements of 20 to 40 nm. The furnished SnO_2 NPs were studied on antibacterial activities by using *Escherichia coli* and *S. aureus*, while antifungal activities were studied by using *Asperjillus nigar* and *T. viridea* which resulted in potential antioxidant activities.

Aloe vera extract was used in a research investigation of SnO_2 NPs that was described by Subramaniam *et al*. (43). The authors suggest two aromatic biomolecules that are possibly involved in the reduction process which, are anthraquinone and glycoside. XRD analysis indicates the crystallite size of SnO_2 NPs as 49 nm while FTIR results proved the presence of Sn-O bond by the appearance of absorption band region 500 cm^{-1}. SEM analysis revealed that the aloe vera solution influences the formation of SnO_2 in which they tend to aggregate, and the particle size becomes larger. No subsequent testing was declared by the author in the articles.

Several biomolecules that serve as the reducing agent in the creation of SnO_2 NPs were discussed by Kandan *et al.* (44). They reported using four types of leaf extract: *Carica papaya*, *Murraya koenigii*, *Moringa oleifera*, and *Acalypha indica*. The biomolecules that were predicted to hold the

function of transformation of tin cation to nanoparticles were flavones, alkaloids, phenols, carbohydrates, and amino acids. From the analysis of XRD, the measurement for the average crystallite size for the four SnO_2 NPs was found to be 5 nm, 19 nm, 38 nm, and 11 nm, whereby they reflected a tetragonal single phase. The authors assumed that the smaller size of SnO_2 NPs produced from the employment of *Carica papaya* extract might be attributed to the better action in controlling the size during the nanoparticle growth. SEM characterization indicates a formation of agglomerated tiny particles with rods. While UV-Vis analysis led to a measurement of the energy band gap with the value of 2.8 to 3.14 eV, which was appropriately carried out for photocatalytic testing. The degradation for all tested photocatalysts on rhodamine-B was found to be almost equal. The summary of the previous works of biosynthesis of SnO_2 NPs using leaves extract are tabulated in Table 1.

Table 1: The biosynthesis of SnO_2 NPs from leaves extract and their testing applications

No	Leaves	Biomolecules responsible	Testing application	Ref.
1	*Daphne mucronata*	Coumarins, coumarino lignans, flavonoids, carboxylic acids, lignin, and triterpenoids	Photocatalytic: 99 % of rhodamine-6G; Antimicrobial: Larger inhibition zones are measured with increased concentration and volume of SnO_2 NPs against GPB, GNB and fungi	32
2	*Pruni spinosae flos*	Flavonoids and phenolic acid	Antimicrobial: Good biocidal effect against GPB, GNB, and fungi. Cytotoxic activity: SnO_2 NPs presence during cell proliferative activity invariably leads to cell death	33
3	*Calotropis gigantea*	Flavonoids, tannins, saponins, terpenoids, alkaloids, and phenols	Photocatalytic: 80% degradation of methyl orange	34
4	*Brassica oleracea L. var. botrytis*	Polyphenol and flavonoid	Photocatalytic: 91 % and 88 % degradation of methylene blue	35
5	*Camellia sinensis*	Epicatechin (EC), epigallocatechin (EGC), picatechin gallate (ECG), and epigallocatechin gallate (EGCG)	N/A	36
6	*Camellia sinensis*	Flavonoids, amino acids, proteins and enzymes	Photocatalytic: 100% degradation of methylene blue and rhodamine-B, 81% degradation of methyl orange	37
7	*Psidium guajava*	Flavonoids, sesquiterpene alcohols, and triterpenoid acids	Photocatalytic: 90% degradation of RY186 dye	38
8	*Aspalathus linearis*	Aspalathin	Photocatalytic: 100% degradation of methylene blue and eosin Y, ~50% of congo red.	39

9	*Plectranthus amboinicus*	Biomolecules not specifically mentioned	Photocatalytic: 95% degradation of rhodamine-B	40
10	*Amaranthus tricolour L*	Gallic acid (3,4,5-OH), myrcetin, quercetin-3-O-rutinoside (rutin), and apigenin-7-O-glucoside (apigetrin)	Photocatalytic: 100% degradation of bromophenol blue	41
11	*Cleistanthus Collinus*	Cleistanthin A and cleistanthin B (lignan lactone glucosides)	Antimicrobial: Larger inhibition zones are measured with increased concentration and volume of SnO_2 NPs against GPB, GNB and fungi	42
12	Aloe vera	Anthraquinone and glycoside	N/A	43
13	*Carica papaya*, *Murraya koenigii*, *Moringa oleifera*, and *Acalypha indica*	Flavones, alkaloids, phenols, carbohydrates, and amino acids	Photocatalytic: 86% degradation of rhodamine-B	44

3.2 The utilization of fruit extract in mediating synthesis

Honarmand *et al*. used *Ziziphus jujube* fruit extract to conduct a biosynthesis of SnO_2 NPs (45). They reported the possible fruit's flavonoids, particularly quercetin, acted as tin cation reducing agent. They also claim this biomolecule prevents the agglomeration of nanoparticles. Analysis from XRD gave a tetragonal rutile structure of SnO_2 NPs with an average crystallite size of about 18 nm. FTIR analysis indicates the presence of SnO_2 NPs by showing an absorption peak corresponding to Sn-OH within the region 1000 to 1100 cm^{-1}. SEM analysis evidenced the formation of nanoparticles with minimal agglomeration. The photocatalytic activity of the SnO_2 NPs was investigated for degradation of two organic dyes which were methylene blue and eriochrome black-T, under direct sunlight. Methylene blue showed better degradation performance by having a 90% result, rather than Eriochrome black-T with 83%. The reusability test recorded four-time cycles of SnO_2 NPs performance that might be attributed to its high stability.

The green synthesis of SnO_2 NPs using *Lycopersicon esculentum* (tomato) peel extract was demonstrated by Garrafa-Galvev *et al.* with different concentrations (46). The authors claim the high percentage of flavonoid content carried a great potential to be acted as the reducing agent in green synthesis. XRD analysis proves SnO_2 NPs in crystalline and tetragonal structures with different sizes and shapes homogeneity attributed to their extract amount. A vibrational peak at 666 cm^{-1} from FTIR analysis proved the presence of the Sn-O-Sn group. TEM images showed the quasi-spherical formation for all nanoparticles NPs, with only slight agglomeration and the sizes were 5.56 nm, 4.67 nm, and 4.01 corresponding to 1%, 2% and 4% samples. UV-Vis analysis translated the result for band gap value and obtained 3.3 eV. Photocatalytic testing recorded 99% degradation performed by SnO_2 NPs with 4% peel extract on methylene blue within 120 min, rather than 67% and 85% degradation

when using SnO_2 NPs with 1% and 2% peel extract.

An extract of the fruit from the *Litsea cubeba* was used by Hong and Jiang to create SnO_2 NPs in their study (47). They believed biomolecules in the fruits especially polyphenols, flavonoids, and other secondary metabolites are the key factors to reduce tin chloride to tin oxide. FTIR analysis confirmed the presence of SnO_2 NPs by showing absorption peaks within 400 to 600 cm^{-1} that belonged to Sn-O and Sn-O-Sn groups. While for morphological proof, SEM demonstrated an irregular shape of nanoparticles, with 40 to 60 nm nanoscale size. The photocatalytic was tested on congo red and recorded a better degradation percentage for SnO_2 NPs annealed at 600^oC rather than 400^oC. The antioxidant study was conducted using SnO_2 NPs based on the DPPH scavenging activity, which indicated a prominent antioxidant capability against DPPH free radicals particularly when using SnO_2 NPs without any thermal treatment with IC_{50} value recorded to be 2257.4 lg/ml.

Senthilkumar and Rajendran described a straightforward, quick, environmentally friendly method for producing SnO_2 thin films utilising *Citrus aurantifolia* (lemon) peel extract (48). This study is based on the justification of the presence of the alkaloid group in lemon to reduce tin oxide. The preparation involved the annealing process at 100 °C and 220 °C. XRD measurement confirmed the tetragonal crystalline structure and high-purity SnO_2 NPs. For SnO_2 thin film annealed up to 100°C, the crystalline size was obtained at 26 nm while for 200 °C the size was 32 nm. FTIR analysis proved the formation of SnO_2 NPs by demonstrating peaks corresponding to O-Sn-O between regions 400 to 600 cm^{-1}. The authors claimed the distribution of the nanostructures was uniform but did not perform any application afterward.

Citrus aurantifolia was reportedly used by Luque *et al*. with various extract strengths (49). Several biomolecules were believed to be present in the fruit extract such as flavonoid-type compounds: rutin, apigenin, hesperetin, nobiletin, kaempferol, and quercetin. In addition, other biomolecules such as flavones, flavanones, naringenin, triterpenoids, and limonoids were also present to aid the biosynthesis mechanism. From the characterization result, FTIR analysis proved the presence of Sn-O-Sn at region 570 to 670 cm^{-1}. While XRD diffraction pattern analysis evidenced the construction of pure SnO_2 NPs with tetragonal structure in the rutile phase. TEM showed the morphology of quasi-spherical formation, and slight agglomeration only happens when using a high concentration of extract. UV-Vis analysis gave band gap measurement within the range of 3.0 to 3.4 eV for the nanoparticles, which later used as the photocatalyst showed a degradation efficiency of 94.4 % on methylene blue within 2 hours.

Subsequently, based on the justification former research papers used biomolecules contained in the plant extract, Luque *et al*. also conducted a synthesis using *Citrus sinensis* to drive the SnO_2 NPs formation (50). The authors did not suggest the name of the biomolecules that are involved in the mechanism but presumed they acted as the reducing agent. FTIR analysis demonstrated absorption peaks at region 1632 cm^{-1} and Sn-O-Sn at 642 cm^{-1} correspond to Sn-O and Sn-O-Sn groups. While XRD evidenced the formation of SnO_2 to be in a tetragonal rutile structure. TEM analysis gave morphology of quasi-spherical with certain agglomeration, and the size was measured as 4.5 nm. UV-Vis analysis facilitated the calculation of the band gap to give a value of 3.49 eV, and this enabled SnO_2 NPs to function as the photocatalyst. The degradation of methylene blue was achieved at 94% within 2 hours.

In addition, Elango and Roopan conducted a study using *Cyphomandra betacea* fruit (51). In this study, the polar biomolecules were pin-pointed to have important action in the mechanism whereby the extraction for the polar biomolecules was carried out using methanol. The volatile compounds like terpenoids, aromatics, esters, and aldehydes were removed primarily. FTIR gave evidence of SnO_2 NPs formation by showing the absorption band of Sn-OH at region 609 cm^{-1} and XRD gave the measurements of the crystallite size as 21 nm. While EDX analysis proved the elemental composition to be 73.57% and 15.75 % for Sn and O. SEM analysis discovered a cluster nanoparticles formation with noticeable sharp edges. The photocatalytic measurements recorded a complete degradation of methylene blue within 70 minutes.

The green process was also reported by Roopan *et al*. using *Annona squamosa* fruit extract (52). The extract was confirmed to possess biomolecules bearing hydroxyl group that accounted to be the capping agent, which later formed a coordination bond with tin cation. XRD analysis indicated the nanoparticles to be a tetragonal crystalline structure with a size of 20 nm and spherical formation of SnO_2 NPs around 27 nm was proved by TEM analysis. The synthesized SnO_2 NPs were tested under a cytotoxicity study using a hepatocellular carcinoma cell line (HepG2), in which the cell morphology correlates with the increment of the nanoparticle's concentrations. The result also indicated cell proliferation with an IC_{50} value of 148 μg/mL, which showed the efficiency of the cytotoxicity using SnO_2 NPs was in moderate average level towards HepG2.

The fabrication of SnO_2 NPs using *Actinidia deliciosa* fruit based on the presence of biomolecules to act as capping and reducing agents such as alkaloids, amino acids, flavonoids, glycosides, and terpenoids has been reported by Gomathi *et al*. (53). From the XRD result, the crystalline structure was discovered to be rutile phase and the average crystallite size was calculated to be 20 nm. FTIR analysis confirmed the presence of Sn-O-Sn and Sn-OH by the appearance of absorption peaks at 500 cm^{-1}, 600 cm^{-1}, and around 1100 cm^{-1}. SEM and TEM analysis evidenced the morphology to be a 5 to 10 nm spherical formation. The photocatalytic testing of the synthesized SnO_2 NPs was carried out to degrade several dyes which were methylene blue, and Methyl orange rhodamine-B which resulted in 89%, 87%, and 97% respectively.

The explanation of the green synthesis of SnO_2 NPs using peel extract from cotton balls was reported by Narasaiah *et al*. (54). The authors did not mention specifically the biomolecules involved in the reaction, but FTIR analysis proved the presence of their functional groups that are responsible for the capping and reducing action, which are hydroxyl groups derived from polyphenols, aromatic amines, and carbonyl. From XRD analysis, it was proven that the crystal structure of SnO_2 NPs is tetragonal with average crystallite size ranging from 4 to 9 nm. TEM demonstrated a spherical formation of samples with an average size of 3.97 nm. EDX gave a measurement of 86.59% tin and 13.41% oxygen to confirm the construction of pure SnO_2 NPs. The photocatalytic testing indicated that the smallest size of SnO_2 NPs effectively degraded methylene blue and methyl orange, and after five consecutive reusability tests it exhibited more than 90% performance. The summary of the previous works of biosynthesis of SnO_2 NPs using leaves extract are tabulated in Table 2.

Table 2: The biosynthesis of SnO_2 NPs from fruits extract and their testing applications

No	Fruits	Biomolecules responsible	Testing application	Ref.
1	*Ziziphus jujube*	Flavonoids (quercetin)	Photocatalytic; 90% degradation of Methylene blue and 83% of Eriochrome black-T	45
2	*Lycopersicon esculentum*	Flavonoids	Photocatalytic; 67% to 99% degradation of methylene blue	46
3	*Litsea cubeba*	Polyphenols and flavonoids	Antioxidant: Strong antioxidant capacity against the DPPH free radical (IC50: 2257.4 µg/mL)	47
4	*Citrus aurantifolia*	Alkaloid	N/A	48
5	*Citrus aurantifolia*	Flavonoids	Photocatalytic; 94.4% degradation of methylene blue	49
6	*Citrus sinensis*	N/A	Photocatalytic; 94% degradation of Methylene blue	50
7	*Cyphomandra betacea*	Terpenoids, aromatics, esters, and aldehydes	Photocatalytic; 100% degradation of methylene blue	51
8	*Annona squamosa*	N/A	Cytotoxic activity: SnO_2 NPs presence during cell proliferative activity invariably leads to cell death	52
9	*Actinidia deliciosa*	Alkaloids, amino acids, flavonoids, glycosides, and terpenoids	Photocatalytic; 89% degradation of methylene blue, 87% of rhodamine-B and 97% of methyl orange	53
10	Cotton balls	N/A	Photocatalytic; 90% degradation of methylene blue and 94% of methyl orange	54

4.0 Conclusion

The present review overviews the utilization of different extracts of leaves and fruits in performing biosynthesis of SnO_2 NPs. This bio-template method is certainly safe, sustainable, economical, and repeatable on a large scale. The function of the biomolecules to act as the capping and reducing agent is very significant to facilitate the formation and control of the size of SnO_2 NPs. Significantly, the hydroxyl group attached to the biomolecules plays an important role in forming the coordination bond through chelating activity. In general, the purely synthesized SnO_2 NPs proved to be worth synthesizing, which demonstrated a unique potential in biological as well as photocatalytic activity. In the future, intensive studies should be conducted to investigate the influence of the different biomolecules on the morphology and size of the produced SnO_2 NPs.

Acknowledgement
The authors would like to acknowledge the Institute of Science UiTM Shah Alam for the provided facilities.

Conflict of interest
Hereby, the authors declare that there is no conflict of interest in the current work.

References

1. Buniyamin I, Akhir RM, Asli NA, Khusaimi Z, and Rusop M. Green synthesis of tin oxide nanoparticles by using leaves extract of *Chromolaena odorata*: The effect of different thermal calcination temperature to the energy band gap. Mater Today Proc. 2022; 1805-1809.

2. Basnet P, Chanu TI, Samanta D, Chatterjee S. A review on bio-synthesized zinc oxide nanoparticles using plant extracts as reductants and stabilizing agents. J. Photochem Photobiol B Biol. 2018; 183: 201-221.

3. Vani P,Manikandan N,Vinitha G. A green strategy to synthesize environment friendly metal oxide nanoparticles for potential applications. Asian J Pharm Clin Res. 2017; 10: 337-343.

4. Schrofel A, Kratošova G, Šafarik I, Šafarikova M, Raška I, Shor LM. Applications of biosynthesized metallic nanoparticles - A review. Acta Biomater. 2014; 10: 4023-4042.

5. Buniyamin I, Eswar KA, Asli NA, Khusaimi Z, Rusop M. Highly-reusable photocatalyst from *Chromolaena Odorata* leaves. APS Proceedings. 2023; 6: 74-78.

6. Buniyamin I, Eswar KA, Mohammad M, Asli NA, Khusaimi Z, Rusop M. Biosynthesized SnO_2 nanoparticles as the effective photocatalyst for water treatment. APS Proceedings. 2023; 7: 58-62.

7. Kumar V, Singh K, Kumar A, Kumar M, Singh K, Vij A, Thakur A. Effect of solvent on crystallographic, morphological and optical properties of SnO_2 nanoparticles. Mater Res Bull. 2017; 85: 202-208.

8. Vijayaraghavan K, Ashokkumar T. Plant-mediated biosynthesis of metallic nanoparticles: A review of literature, factors affecting synthesis, characterization techniques and applications. J Environ Chem Eng. 2017; 5: 4866-4883.

9. Gorai S. Bio-based synthesis and applications of SnO_2 nanoparticles-An overview. J Mater Environ Sci. 2018; 9: 2894-2903.

10. Murzalinov D, Dmitriyeva E, Lebedev I, Bondar EA. The effect of pH solution in the sol-gel process on the structure and properties of thin SnO_2 films. Processes. 2022; 10: 1116.

11. Kim H, Son JH, Bae D. Synthesis and characterization of SnO_2 nanoparticles by hydrothermal processing. Kor J Mater Res. 2011; 21: 415-418.

12. Ahmad W, Pandey A, Rajput V, Kumar V, Verma M, Kim H. Plant extract mediated cost-effective tin oxide nanoparticles: A review on synthesis, properties, and potential applications. Curr Res Green Sustain Chem. 2021; 4: 100211.

13. Matussin S, Hilni Harunsani M, Tan AL, Khan MM. Plant-extract-mediated SnO_2 nanoparticles: Synthesis and applications. ACS Sustain Chem Eng. 2020; 8: 3040-3054.

14. Buniyamin I, Akhir RM, Asli NA, Malek MF, Khusaimi Z, Mahmood MR. Nanotechnology applications in biomedical systems. Curr Nanomater. 2022; 7: 167-180.

15. Ayeshamariam A, Vidhya VS, Sivaranjani S, Bououdina M, PerumalSamy R, Jayachandran M. Synthesis and characterizations of SnO_2 nanoparticles. J Nanoelectron Optoelectron. 2013; 8: 1-8.

16. Naje AN, Norry AS, Suhail AM. Preparation and characterization of SnO_2 nanoparticles. Int J Innov Res Technol Sci Eng. 2013; 2: 7068-7072.

17. Harisha Kumar K, Kumar P, Dharmaprakash SM. Influence of substrate temperature and laser wavelength on the structural, optical and electrical properties of laser ablated tin oxide thin films. IOP Conf Ser Mater Sci Eng. 2022; 1221: 012023.

18. Patil GE, Kajale DD, Chavan DN, Pawar NK, Ahire PT, Shinde SD, Gaikwad VB, Jain GH. Synthesis, characterization and gas sensing

performance of SnO_2 thin films prepared by spray pyrolysis. Bull Mater. Sci. 2011; 34: 1-9.

19. Nehru LC, Sanjeeviraja C. Rapid synthesis of nanocrystalline SnO_2 by a microwave-assisted combustion method. J Adv Ceram. 2014; 3: 171-176.

20. Gebreslassie YT, Gebretnsae HG. Green and cost-effective synthesis of tin oxide nanoparticles: A review on the synthesis methodologies, mechanism of formation, and their potential applications. Nanoscale Res Lett. 2021; 16: 97.

21. Kavitha KS, Syed Baker, Rakshith D, Kavitha HU, Yashwantha Rao HC, Harini BP, Satish SI. Plants as green source towards synthesis of nanoparticles. Int Res. J Biological Sci. 2013; 2: 66-76.

22. Zwanida NN. A review on the extraction methods use in medicinal plants, principle, strength and limitation. Int J Med Aromat Plants. 2015; 4: 1962015.

23. Mohamad NAN, Nur Arham A, Jai J, Hadi A. Plant extract as reducing agent in synthesis of metallic nanoparticles: A review. Adv Mat Res. 2014; 832: 350-355.

24. Buniyamin I, Akhir RM, Nurfazianawatie MZ, Omar H, Malek NSA, Rostan NF, Eswar KA, Rosman NF, Abdullah MA, Asli NA, Khusaimi Z, Rusop M. *Aquilaria malaccensis* and *Pandanus amaryllifolius* mediated synthesis of tin oxide nanoparticles: The effect of the thermal calcination temperature. Mater Today. 2023; 75: 23-30.

25. Buniyamin I, Md Akhir R, Asnida Asli N, Khusaimi Z, Rusop Mahmood M. Biosynthesis of SnO_2 nanoparticles by aqueous leaves extract of Aquilaria Malaccensis (agarwood). IOP Conf Ser Mater Sci Eng. 2021; 1092: 012070.

26. Ahmed S, Annu, Chaudhry SA, Ikram S. A review on biogenic synthesis of ZnO nanoparticles using plant extracts and microbes: A prospect towards green chemistry. J Photochem Photobiol B, Biol. 2017; 166: 272-284.

27. Buniyamin I, Md Akhir R, Asnida Asli N, Khusaimi Z, Rusop M. Effect of calcination time on biosynthesised SnO_2 nanoparticles using bioactive compound from leaves extract of *Chromolaena odorata* effect of calcination time on biosynthesised SnO_2 nanoparticles using bioactive compound from leaves extract of *Chromolaena*. AIP Conf Proc. 2021; 1092: 020006.

28. Gawade VV, Gavade NL, Shinde HM, Babar SB, Kadam AN, Garadkar KM. Green synthesis of ZnO nanoparticles by using *Calotropis procera* leaves for the photodegradation of methyl orange. J Mater Sci Mater Electron. 2017; 28: 14033-14039.

29. Jain S, Mehata MS. Medicinal plant leaf extract and pure flavonoid mediated green synthesis of silver nanoparticles and their enhanced antibacterial property. Sci Rep. 2017; 7: 15867.

30. Fatimah I, Sahroni I, Muraza O, Doong R. One-pot biosynthesis of SnO_2 quantum dots mediated by *Clitoria ternatea* flower extract for photocatalytic degradation of rhodamine B. J Environ Chem Eng 2020; 8: 103879.

31. Danhalilu RL, Kankara AI, Batagarawa SM. Green synthesis of metallic nanoparticles using leaf extract of *Calotropis* species and their applications: A review. Curr Appl Sci Technol. 2019; 32: 1-10.

32. Haq S, Rehman W, Waseem M, Shah A, Khan AR, Rehman MU, Ahmad P, Khan B, Ali G. Green synthesis and characterization of tin dioxide nanoparticles for photocatalytic and antimicrobial studies. Mater Res Express. 2020; 7: 025012.

33. Dobrucka R, Dlugaszewska J, Kaczmarek M. Cytotoxic and antimicrobial effect of biosynthesized SnO_2 nanoparticles using *Pruni spinosae* flos extract. Inorg Nano-Met Chem. 2019; 48: 367-376.

34. Bhosale TT, Shinde HM, Gavade NL, Babar SB, Gawade VV, Sabale SR, Kamble RJ, Shirke BS, Garadkar KM. Synthesis of SnO_2 nanoparticles by aqueous leaf extract of *Calotropis gigantea* for photocatalytic

applications. J Mater Sci Mater Electron. 2018; 1-10.

35. Osuntokun J, Onwudiwe DC, Ebenso EE. Synthesis and photocatalytic properties of SnO_2 nanoparticles prepared using aqueous extract of cauliflower. J Clust Sci. 2017; 1-14.

36. Selvakumari JC, Ahila M, Malligavathy M, Pathinettam Padiyan D. Structural, morphological, and optical properties of tin (iv) oxide nanoparticles synthesized using *Camellia sinensis* extract: a green approach. Int J Miner Metall Mater. 2017; 24: 1043-1051.

37. Luque PA, Chinchillas-Chinchillas MJ, Nava O, Lugo-Medina E, Martínez-Rosas ME, Carrillo-Castillo A, Vilchis-Nestor AR, Madrigal-Mu˜noz LE, Garrafa-G´alvez HE. Green synthesis of tin dioxide nanoparticles using *Camellia sinensis* and its application in photocatalytic degradation of textile dyes. Optik. 2021; 229.

38. Kumar M, Mehta A, Mishra A, Singh J, Rawat M, Basu S. Biosynthesis of tin oxide nanoparticles using *Psidium guajava* leave extract for photocatalytic dye degradation under sunlight. Mater Lett. 2017; 215: 124-125.

39. Diallo A, Manikandan E, Rajendran V, Maaza M. Physical & enhanced photocatalytic properties of green synthesized SnO_2 nanoparticles via *Aspalathus linearis*. J Alloys Compd. 2016; 681: 561-570.

40. Fu L, Zheng Y, Ren Q, Wang A, Deng B. Green biosynthesis of SnO_2 nanoparticles by *Plectranthus amboinicus* leaf extract their photocatalytic activity toward rhodamine B degradation. J Ovonic Res. 2015; 11: 21-26.

41. Wicaksono WP, Sahroni I, Saba AK, Rahman R, Fatimah I. Biofabricated SnO_2 nanoparticles using red spinach (*Amaranthus tricolor* L.) extract and the study on photocatalytic and electrochemical sensing activity. Mater Res Express. 2020; 7: 075009.

42. Kamaraj P, Vennila R, Arthanareeswari M, Kala SD. Biological activities of tin oxide nanoparticles synthesized using plant extract. J Pharm Pharm Sci. 2015; 3: 382-388.

43. Veeraganesha V, Subramaniyan A, Sornakumar T. Effect of Aloevera on synthesis of nano tin (iv) oxide. Asian J Nanosci Mater. 2018; 1: 115-121.

44. Sundara Selvam PS, Ganesan D, Rajangam V, Raji A, Kandan V. Green synthesis of SnO_2 Nanoparticles for catalytic degradation of rhodamine B. Iran J Sci Technol Trans A Sci. 2020; 44: 661-676.

45. Honarmand M, Golmohammadi M, Naeimi A. Biosynthesis of tin oxide (SnO_2) nanoparticles using jujube fruit for photocatalytic degradation of organic dyes. Adv Powder Technol. 2019; 30: 1551-1557.

46. Garrafa-Galvez HE, Nava O, Soto-Robles CA, Vilchis-Nestor AR, Castro-Beltran A, Luque PA. Green synthesis of SnO_2 nanoparticle using Lycopersicon Esculentum peel extract. J Mol Struct. 2019; 1197: 354-360.

47. Hong GB, Jiang CJ. Synthesis of SnO_2 nanoparticles using extracts from Litsea cubeba fruits. J Nanosci Nanotechnol. 2018; 18: 5020-5025.

48. Senthilkumar S, Rajendran A. Eco-friendly synthesis and characterization of nanostructure SnO_2 thin films using Citrus Aurantifolia peel extract by spin coating method. J Nanomed Res. 2017; 6: 4.

49. Luque PA, Nava O, Soto-Robles CA, Garrafa-Galvez HE, Martinez-Rosas ME, Chinchillas-Chinchillas MJ, Vilchis-Nestor AR. Castro-Beltran A. SnO_2 nanoparticles synthesized with *Citrus aurantifolia* and their performance in photocatalysis. J Mater Sci Mater Electron. 2020; 31: 16859-16866.

50. Luque PA, Navaa O, Soto-Roblesa CA, Chinchillas-Chinchillas MJ, Garrafa-Galvez HE, Baez-Lopeza YA, Valdez-Núñezc KP, Vilchis-Nestord AR, Castro-Beltrán A. Improved photocatalytic efficiency of SnO_2 nanoparticles through green synthesis. Optik. 2020; 206: 164299.

51. Elango G, Roopan SM. Efficacy of SnO_2 nanoparticles toward photocatalytic degradation of methylene blue dye. J Photochem Photobiol B, Biol. 2016; 155: 34-38.

52. Roopan SM, Suthindhiran KS, Madhumitha G, Suthindhiran K. Biogenic-Production of SnO_2 Nanoparticles and its cytotoxic effect against hepatocellular carcinoma cell line (HepG2). Appl Biochem Biotechnol. 2015; 2: 1567-1575.

53. Gomathi E, Jayapriya M, Arulmozhi M. Environmental benign synthesis of tin oxide (SnO_2) nanoparticles using *Actinidia deliciosa* (Kiwi) peel extract with enhanced catalytic properties. Inorg Chem Commun. 2021; 130: 108670.

54. Narasaiah BP, Banoth P, Sohan A, Mandal BK, Bustamante Dominguez AG, De Los Santos Valladares L, Kollu P. Green biosynthesis of tin oxide nanomaterials mediated by agro-waste cotton boll peel extracts for the remediation of environmental pollutant dyes. ACS Omega. 2022; 7: 15423-15438.